MECHANISTIC STUDIES OF OXIDE ELECTRODES REVERSIBLY INCORPORATING Li$^+$ IONS

GIANFRANCO PISTOIA

Centro di Studio per la Elettrochimica e la Chimica Fisica delle Interfasi del C.N.R., Via del Castro Laurenziano 7, 00161 Rome (Italy)

Summary

Transition metal oxides capable of reversibly incorporating Li$^+$ ions are examined with particular emphasis on their structural features. The thermodynamic, kinetic, and electrochemical aspects of the insertion processes are also discussed.

---

1. Introduction

In Whittingham's comprehensive review of the chemistry of intercalation compounds, a number of oxides was included along with layered transition metal chalcogenides [1]. However, the former were dealt with relatively briefly due to a better characterization of the latter in structural, thermodynamic, kinetic, and electrochemical terms. In the last few years, the leadership of chalcogenides in the field of secondary Li cells has been challenged. Indeed, some of them, *e.g.*, TiS$_2$, show excellent reversible behaviour and may sustain deep cycles at high c.d. However, it cannot be denied that for TiS$_2$ there exist a number of significant drawbacks, such as:

(1) the need to prepare a very pure compound of exact stoichiometry (at high cost);

(2) sensitivity to moisture;

(3) relatively low energy density due to the weight of S;

(4) sloping discharge curve, typical of single phase intercalation processes;

(5) possibility of solvent co-intercalation in the layered structure.

Metal oxides offer an alternative to chalcogenides and provide a range of compounds which may, to varying extents, alleviate the drawbacks listed above, although none of those tested so far can compete with TiS$_2$ in terms of rate capability [1].

The recent discovery of materials which, as in the case of V$_6$O$_{13}$ [2, 3], show efficient rechargeability in long cycling tests, has stimulated a new wave of basic studies on metal transition oxides. A great deal of new data on crystallographic structures, kinetics of Li$^+$ diffusion, electronic configura-

tions, thermodynamics, and electrochemistry in a non-aqueous media is now appearing in the literature. Thus, the gap between oxides and chalcogenides is rapidly being filled.

It is the aim of this paper to collect and summarize the relevant information on the mechanisms through which solid oxides can reversibly incorporate Li^+ ions. In this respect, not only the compounds showing promise as cathode materials for Li cells but also some of those having features of particular interest have been taken into account.

2. Structures and related sites for Li^+

Transition metal oxides are known to exist in a variety of structures which can be broadly classified into layered and tridimensional (framework) structures. Unlike the dichalcogenides, the number of two-dimensional oxides with van der Waals bonded layers, useful as reversible cathodes, is small. Molybdenum trioxide [1, 4, 5], $Mo_{18}O_{52}$ [5] and Li_xCoO_2 [6] provide the most significant examples. On the contrary, oxides with host lattices bonded in three dimensions form a large class.

2.1. Layered oxides

The insertion process in layered oxides does not seem to be as smooth as those reported for most of the layered dichalcogenides [1]. First, the interlayer separation is larger than that observed for the latter class ($b/2$ increases by 0.96 Å in $LiMoO_3$ [4] and 1.13 Å in $Li_{12.6}Mo_{18}O_{52}$ [7], as compared with 0.50 Å in $LiTiS_2$ [1]). Secondly, the structures tend to reveal various degrees of reorganization, as shown by X-ray analyses for MoO_3 and $Mo_{18}O_{52}$ [1, 7]. For Li_xCoO_2 [6] such structural alterations are not mentioned in the preliminary diffractometric data, but the abrupt change of the slope of the OCV/x curve at $x \simeq 0.7$ makes them highly probable for this compound too. It is obvious from these results that layered oxides cannot be included in the group of true intercalation compounds [8]. Their inclusion in the more extended class of insertion compounds seems more appropriate. Structural changes may be connected, at least for the better characterized Mo oxides, with marked distortion in the structures [9] which make pathways and sites for Li^+ non-equivalent. Further distortions may then occur (especially at high Li^+ content) from which the formation of new phases and kinetically difficult re-oxidation ensues.

No direct data have been obtained for Li^+ coordination in the Mo oxides, whereas in Li_xCoO_2, Li^+ ions are reported to reside in octahedral sites of the basic $CdCl_2$ structure. On the basis of the amount of Li^+ inserted in $Mo_{18}O_{52}$, a tetrahedral coordination was supposed at least for high Li^+ contents [5].

2.2. Framework oxides

Transition metals tend to coordinate 6 oxygen atoms, giving MO_6 octahedra which are the most common building units of the structures here

considered. These units may simply be connected through corner sharing, so giving ReO_3-related structures, or by edge and corner sharing as, for instance, in V_2O_5 and rutile TiO_2. The resulting structures are characterized by the presence of channels running in one (TiO_2), two (V_2O_5) or three (ReO_3) directions. In these channels, Li^+ ions find their way to coordination sites within the cavities whose shapes and sizes are related to the dimensions and connections of octahedra.

2.2.1. TiO_2 (rutile)-related structures

These structures are ideally described as an h.c.p. oxygen lattice based on edge sharing octahedra forming infinite chains in one direction. These chains are linked by corner sharing, thus forming unidirectional channels (Fig. 1) containing one octahedral or two tetrahedral sites for Li^+. Murphy *et al.* [10, 11] have investigated several rutile-type oxides and found that their ability to insert Li^+ correlates with unit cell volume and electronic conductivity. A good electronic conductivity helps screening repulsion forces among Li^+, thus facilitating insertion. A large cell volume corresponds to large channel sizes. Hong [12] has pointed out that, from a geometrical point of view, the bottleneck formed by a square planar array of oxygen ions is usually sufficient to allow jumping of Li^+ from site to site. For the rutiles the situation is somewhat less favourable because each Li^+ has to pass through a transition state based on three oxygen ions.
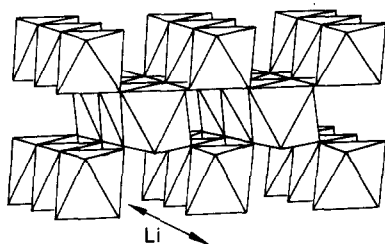

Fig. 1. Rutile structure showing channels along [001] for Li^+ diffusion (ref. 11).

Therefore, only rutile-type structures with (relatively) large channels may incorporate appreciable amounts of Li^+, although notable exceptions are known, such as that provided by NbO_2. In this case, the lack of electronic conductivity has overwhelmed geometric factors.

This class of compounds, although interesting for providing examples of unidirectional channels giving (to a various extent) hospitality to Li^+ ions, has, in fact, given no materials useful for battery application.

2.2.2. ReO_3-related structures

A class of compounds far more interesting as potential hosts in practical rechargeable Li cells is formed by those based on the ReO_3 structure. The latter is formed by ReO_6 octahedra extending in all three directions through corner sharing only. This manner of connection produces cavities in the

structure having a shape which, as noted by Murphy [11, 13], is similar to that of perovskite ($CaTiO_3$). Figure 2(a) shows how the octahedra may generate such a cavity. Connection of the square faces of the cavities produces channels which, for ReO_3, run in three perpendicular directions and are expected to ensure fast Li^+ motion. However, it has been demonstrated that cubic ReO_3, upon acceptance of more than 1 Li^+/mol, turns to rhombohedral $LiReO_3$ and Li_2ReO_3 phases [14, 15]. This transformation accounts for the slow electrochemical Li^+ uptake/removal [13] and has been explained on the basis of a twisting of the ReO_3 lattice about the shared corners [15], as is shown in Fig. 2(b). This twist transforms a 12 coordinate cavity into two 6 coordinate octahedral cavities sharing faces. The occurrence of such a peculiar phenomenon is only made possible by the extreme flexibility of a structure in which the building units are only corner shared. By introducing edge sharing in it, twisting may be largely controlled and the structure stability enhanced, although the directions for Li^+ diffusion reduce from 3 to 2 (Fig. 2(c)) or even 1.

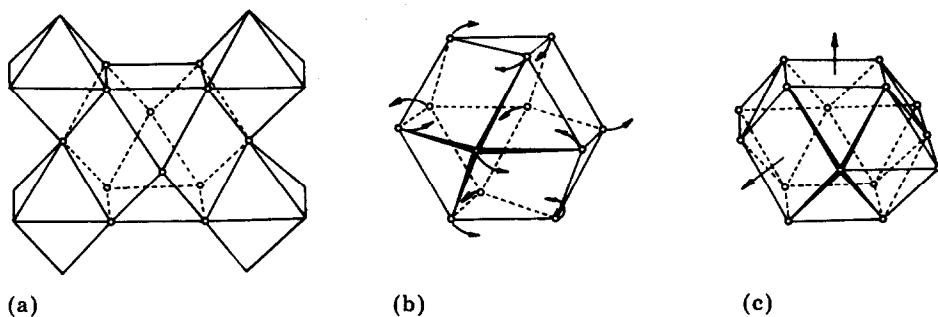(a)   (b)   (c)

Fig. 2. (a) Perovskite-like cavity formed by corner sharing octahedra (only the lateral octahedra are reported for clarity); (b) twisting of type (a) cavity in $LiReO_3$ (ref. 15); (c) cavity of V_6O_{13} (ref. 13).

Edge sharing in ReO_3-related structures may be induced by shear mechanisms, as observed in the Mo_nO_{3n-1} series [9], in the V oxides (V_2O_5, V_6O_{13} and VO_2) [3, 13, 16] and in the mixed oxides FeV_3O_8 [15] and $(Mo_{0.3}V_{0.7})_2O_5$ [17]. Some of these compounds are among the most efficient reversible cathodes for Li cells.

The Mo oxides, i.e., Mo_8O_{23}, Mo_9O_{26} and Mo_4O_{11}, recently investigated at the Bell Laboratories [18] and in the author's laboratory [19 - 21] may be thought of as constituted by slabs, n octahedra thick, which are mutually connected by octahedra sharing edges in Mo_8O_{23} and Mo_9O_{26} [9]. In these structures, the perovskite-like cavities are tridirectional both within the slabs and at the slab boundaries, although some cavities are larger and provide a further direction [7]. Investigation of the reversibility of Mo_8O_{23} [20, 21] has shown that Li^+ diffuses rapidly in the four sided channels (at least 2.8 Å wide) running through the square or rectangular faces of the cavities. Some structural reorganizations occur in the $0.0 < x < 0.8$ range ($x = Li^+$/Mo), as

evidenced, among other results, by a structure contraction, similar to that observed for ReO_3 [14], at $x < 0.2$. This contraction occurs because the 12 - 14 coordinate cavities are larger than those required by Li^+ at low x values. A major reorganization occurs at $x > 0.8$ which makes reoxidation beyond this value difficult.

The V oxides may be thought of as derived from ReO_3 by a first shear (V_2O_5) or a second shear (V_6O_{13} and VO_2) mechanism, as shown in Fig. 3 [3]. The structure of V_6O_{13}, the most interesting of the three from an electrochemical viewpoint, contains edge shared octahedra forming single and double zig-zag chains linked together by further edge sharing. The resulting sheets (single and double) are interconnected by corner sharing, thus giving a tridimensional framework.
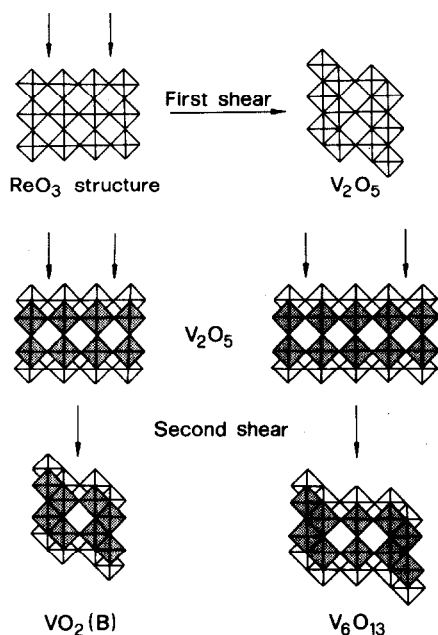

Fig. 3. Formation of V_2O_5 (first shear) and of V_6O_{13} and VO_2 (second shear) from ReO_3. The arrows indicate the shear planes (ref. 3).

By thermal decomposition of NH_4VO_3, a slightly non-stoichiometric material (V_6O_{13+x}, with $x \leqslant 0.2$) may be prepared, which also shows a good performance as a cathode for secondary Li batteries [2, 3]. Structurally, this compound is supposed to differ from the stoichiometric one by inserting an extra double sheet of VO_2 in the V_6O_{13} structure [3, 22]. Due to the small number of foreign sheets (<1.5%) the powder X-ray diffraction patterns for stoichiometric and nonstoichiometric V_6O_{13} closely resemble each other. It will be shown later that both structures tend to reorganize by Li^+ insertion,

as shown by the stepped OCV/x curves and, for V_6O_{13+x}, by a first charge curve less efficient than the discharge curve [2, 3]. This, however, does not prevent these oxides from showing a good cycling behaviour, provided the lower voltage limit is kept above ca. 1.7 V to avoid irreversible structural changes [2]. The cavities present in the framework structure of V_6O_{13} are of the perovskite-type (Fig. 2(c)) with 3 faces capped by oxygen and 2 directions for Li^+ motion. It has been supposed that 4 Li^+ ions are taken in each cavity [13], each coordinating 5 oxygen ions in a square pyramidal arrangement [23].

Very recently, in the author's laboratory, $Li_{1+x}V_3O_8$ cathodes have been tested whose structure is closely related to that of V_6O_{13} [24]. This phase may be considered as consisting of double and single zig-zag strings of highly distorted octahedra arranged so as to provide octahedral and tetrahedral sites for Li^+. Its electrochemical performance (for low x values in the initial cathode material) can overcome that reported for stoichiometric V_6O_{13}.

The mixed oxide $(Mo_{0.3}V_{0.7})_2O_5$ is an interesting material not only for giving a good performance in Li batteries [25, 26], but also for some structural considerations. Indeed, its lattice is built in exactly the same way as that of V_2O_5 [17], with MO_6 octahedra sharing edges to form chains interconnected by sharing corners. However, V_2O_5 can only accept 1 Li^+/mol before its structure collapses due to a breaking of the long V–O bond [13]. In $(Mo_{0.3}V_{0.7})_2O_5$ the long bond along the b axis is sufficiently shorter than that of V_2O_5 to prevent cleavage of the structure. In this way, more than 2 Li^+/mol may be reversibly inserted in the lattice [25, 26]. The metal–oxygen distances therefore play a fundamental role from the point of view of bottleneck size [12] and structure stability.

2.2.3. Hexagonal structures

Corner sharing between octahedra does not necessarily give rise to an ReO_3-type structure. An interesting example is given by the recently prepared hexagonal WO_3, in which the WO_6 octahedra are connected in such a way as to form a wide, hexagonal channel running through the structure [27]. In the hexagonal tungsten bronzes this channel is partly filled by such ions as K^+ or NH_4^+ [27], but these ions are not strictly necessary for the hexagonal structure to exist. Apart from h-WO_3, two other hexagonal oxides, $MoW_{11}O_{36}$ and $MoW_{14}O_{45}$ [28], have been prepared. What is interesting about these compounds endowed with large tunnels is the capability of accepting considerably higher amounts of Li^+ than their perovskite-like counterparts. Monoclinic WO_3, having the typical ReO_3 structure, may only intercalate 0.67 Li^+/W [29], whereas h-WO_3 accepts 2 Li^+/W [27]. The latter figure also pertains to $(NH_4)_{0.33}WO_3$, which is also hexagonal [29].

So far, there are no reports on the speed of Li^+ diffusion in these compounds and on structural variations as a function of Li^+/W. Conversely, a deep investigation of the phase diagram of Li_xWO_3 has been obtained for the monoclinic variety [29].

2.2.4. Mixed polygonal networks

The above mentioned Mo−W oxides can also be included in the family of structures formed by different types of polyhedra. These are connected in two dimensions, forming polygonal networks in which tunnels with 3 to 6 sides are enclosed [9]. Some Mo and W oxides, already tested as cathodes for Li batteries, also belong to this group, i.e., $Mo_{17}O_{47}$, Mo_5O_{14} [18, 19] and $W_{18}O_{49}$ [30]. The first has recently been reported to be the best among non-stoichiometric Mo oxides [18].

2.2.5. MnO_2

This material is linked with the spread of Li batteries in the market. However, little is known about the mechanistic aspects of Li^+ incorporation in its structure. As a matter of fact, it should be more appropriate to refer to 'structures' even when dealing with γ-MnO_2 only, i.e., the starting material for cathodes of both aqueous and non-aqueous cells. However, the basis of all these 'structures' is constituted by a ramsdellite matrix (double chains of edge shared MnO_6 octahedra) containing random domains of pyrolusite (single chains of edge shared octahedra) [31], as shown in Fig. 4.

On heating, these structures alter to form so-called γ/β and $\bar{\beta}$ phases [32]. The γ/β phase has been found to be the most efficient [33, 34] in terms of capacity and energy density. Why the latter outperforms the β phase is at present not clearly understood. Voinov [35] has shown that in γ/β-MnO_2, Li^+ occupy corner shared tetrahedral sites only. The reversibility of this process has received little attention so far. In preliminary experiments carried out in this laboratory, it has been observed that a γ/β phase cycles in a less satisfactory way than a γ phase (Fig. 5), thus confirming the findings of others [36]. This result is in agreement with X-ray analyses showing substantial structure retention during Li^+ insertion for γ-MnO_2 and significant alterations for γ/β-MnO_2 [32]. However, the rationale for this pattern is presently unavailable.
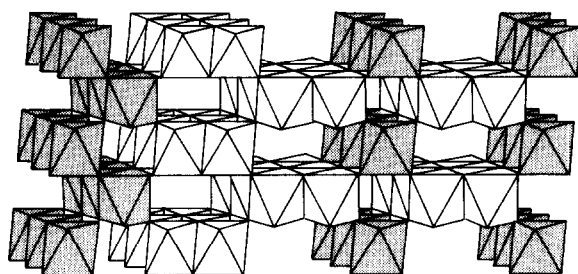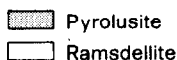

Representative nsutite

▨ Pyrolusite
▢ Ramsdellite

Fig. 4. Idealized representation of the nsutite (γ-MnO_2) structure. Pyrolusite domains indicated by dotted octahedra (ref. 31).
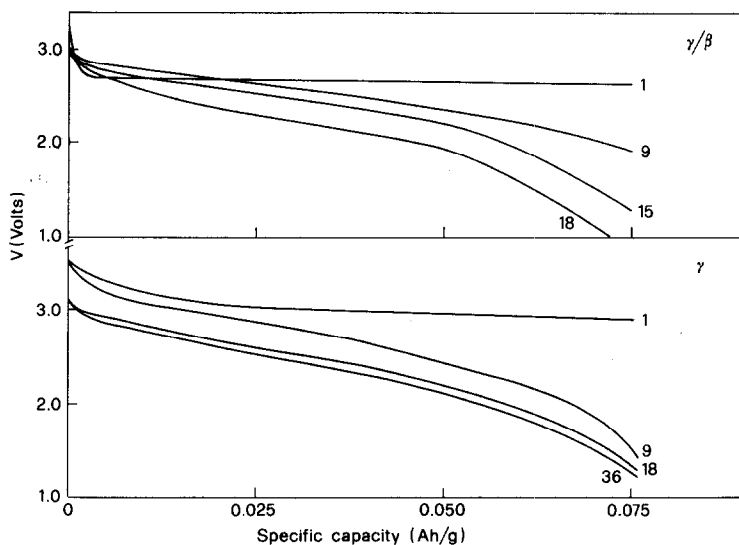
Fig. 5. Cycling of Li/MnO$_2$ cells at 1 mA/cm^2 and 25% d.o.d.

3. Kinetics

Many of the oxides reported in the previous section have shown a high velocity of Li$^+$ diffusion in their lattices. This stems from their fulfilling two key requirements, *i.e.*, sufficiently large bottlenecks within sites and little disposition to form covalent Li–O bonds [12]. In all compounds containing perovskite-like cavities the bottleneck is a square planar array (sometimes distorted) of oxygen ions. The sides of this square are large enough (~ 2.8 Å) for the nonstoichiometric Mo oxides [9] and for the V oxides shear-related to ReO$_3$ [13]. However, geometrical factors should be insufficient to permit fast Li$^+$ diffusion if strong Li–O interactions should occur. The degree of covalency of the Li–O bond has to be low, this occurring when the number of M–O bonds of the original lattice is high enough. For Li$^+$ a high mobility is possible when oxygen is coordinated with at least 3, and preferably 4, metal ions. In WO$_3$ and ReO$_3$, where only corner sharing occurs between octahedra, O^{2-} are bonded to 2 cations; this explains the slow rate of diffusion. Dickens reports $\tilde{D} = 2.8 \times 10^{-11}$ cm^2 s^{-1} for Li$_{0.26}$WO$_3$ [37].

In the shear V oxides such as V$_6$O$_{13}$ and V$_2$O$_5$, the O^{2-} along the shear planes are bonded to 3 cations and, indeed, higher chemical diffusion coefficients have been measured. For Li$_x$V$_6$O$_{13}$ (0.0 < x < 2.5) $\tilde{D}$ values in the range 10^{-8} - 10^{-9} cm^2 s^{-1} have been found [22, 37]. Li$_x$V$_2$O$_5$ (0.01 < x < 0.98) also shows values of 10^{-8} cm^2 s^{-1} [37].

These considerations also apply to Mo$_8$O$_{23}$ for which $\tilde{D}$ values of the order of 10^{-9} cm^2 s^{-1} in all the reversible insertion ranges [7] have been measured.

In $Li_{1+x}V_3O_8$ some O^{2-} are linked to Li^+ in the rigid network, so increasing the number of their M–O bonds. This reduces the number of sp^3 orbitals available for bonding Li^+ ions entering the lattice and the Li^+ diffusivity is enhanced. Indeed, Li cells based on this material have shown quite high rate capabilities.

In the rutiles each O^{2-} is linked to 3 cations, but some of them fail to incorporate significant amounts of Li^+. This has been connected with reduced channel sizes (and, hence, cell volumes), as in the cases of VO_2 and MnO_2 [10, 11]. It may be stated that above *ca.* 60 Å rutiles may accept substantial amounts of Li^+. However, there are important exceptions, such as NbO_2 and, in part, TiO_2. These compounds are characterized by a low electronic conductivity so that screening of the coulombic repulsion between Li^+ ions [10, 11] is limited. Of course, several oxides, such as anatase TiO_2 or γ-MnO_2 are poor conductors and, nevertheless, incorporate useful amounts of Li^+. Therefore, electronic conductivity appears to be strictly necessary only in connection with a reduced cell volume (narrow channels).

It is worthy of note that none of the layered oxides for which $\widetilde{D}$ has been measured shows faster diffusions than those of framework oxides. For Li_xCoO_2 ($0.2 < x < 0.8$) [6], $Li_{3.6}Mo_{18}O_{52}$ [7] and $Li_{0.3}MoO_3$ [37] $\widetilde{D}$ values of the order of 10^{-9} cm^2 s^{-1} have been found. On the contrary, for Na (cubic) and K (hexagonal) tungsten bronzes, where optimum geometrical and electronic conditions exist for Li^+ motion, values of 10^{-7} cm^2 s^{-1} have been measured at moderate Li^+ contents [38].

4. Thermodynamics

Accurate phase diagrams have been obtained for different Li–metal oxide systems, and attempts have been made to separate the contribution of the various thermodynamic parameters from the chemical potentials (or free energies) of the insertion processes.

All the E/x curves for oxides (perhaps with the exception of cubic W bronzes [38]) have non-linear trends, with steps of different length and deepness indicating various degrees of structural reorganization. In this sense a typical curve is shown by $Li_xV_2O_5$ (Fig. 6), where single and double phase regions smoothly alternate [39]. This indicates that almost all the metal oxides (including the layered ones) belong to the broad family of insertion compounds rather than the more restricted one of true intercalation compounds.

Li^+ occupation of different crystallographic sites, as in Mo_8O_{23} [7] and in $K_{0.3}WO_3$ [38], also contributes to give complex E/x profiles.

For an electrode in which Li^+ dissolves E is generally given by the expression $E = (1/F)\Delta\mu_{Li^+}$ [40], where $\Delta\mu$ is the Li^+ chemical potential difference between a cathode and a reference electrode.
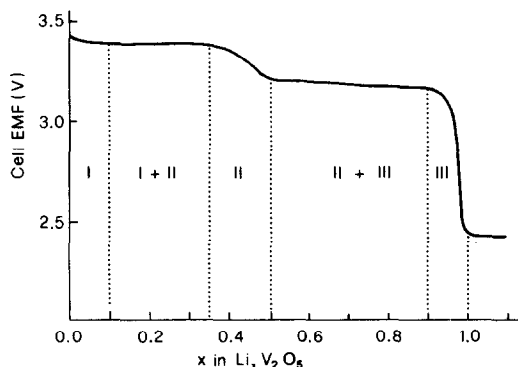
Fig. 6. E/x curve for Li/Li$_x$V$_2$O$_5$ cells (ref. 3).

The contributions to μ_{Li^+} may generally be listed as follows:
(1) interaction energy among inserted ions;
(2) variation of the electron chemical potential;
(3) entropy of filling vacant sites;
(4) lattice expansion energy [41].
Terms (3) and (4) give limited contributions to μ in transition metal oxides apart from initial and final insertion values. Indeed, Dickens has found small entropic contributions for several oxides [37] since the reactions only involve solid components. The same result has been obtained by Huggins [38] for cubic W bronzes. More substantial contributions come from terms (1) (as, for instance, in Mo$_{18}$O$_{52}$ [7]) and (2) (as for Na$_x$WO$_3$ [38]).

Measurements of the enthalpy of insertion of Li$^+$ in several oxides have been recently carried out [37, 42]. $\Delta H/x$ values give a measure of the binding energy of Li$^+$ in the host lattice. They also correlate (for a given x) to the oxidizing power of the oxides. Thus, for instance, the order has been found: $\Delta H_{V_2O_5} > \Delta H_{MnO_2} > \Delta H_{MoO_3} > \Delta H_{WO_3}$. For a given oxide, ΔH decreases, as x increases, by an amount which gives an indication of the structural disturbance induced by Li$^+$. For instance, in Li$_x$V$_2$O$_5$ $(0.5 < x < 1.0)$ for successive phases ΔH decreases by less than 5% [42]. In Li$_x$V$_6$O$_{13}$ ΔH changes by 7% from $x = 0.70$ to $x = 2.82$ [37], but for monoclinic WO$_3$, which is known to undergo several phase changes [29], the ΔH change is 20% $(0.084 < x < 0.71)$ [37].

Voltage steps, provided the differences in the energy contributions are not too large, do not prevent efficient Li$^+$ de-intercalation. There are many examples of this behaviour, one being provided by non-stoichiometric V$_6$O$_{13}$ (Fig. 7) [2]. On charging, 15 - 20% of the initial capacity is lost, but after the second cycle the situation tends to level off and high re-charge efficiencies may be obtained.
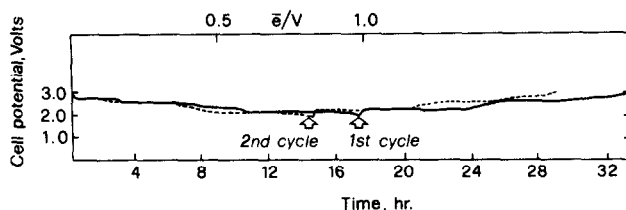
Fig. 7. 1st and 2nd cycle for non-stoichiometric V_6O_{13} at 0.5 mA/cm^2 (ref. 2).

5. Electrochemical features

From a thermodynamic and kinetic point of view, many transition metal oxides appear to be potentially useful cathodes for secondary Li battery applications. As a matter of fact, only few of them can be classed as prospective materials, *i.e.*, those showing high energy densities, electrolyte compatibility and reduced performance losses during extended cycling. Table 1 summarizes some interesting oxides. It is immediately apparent that their energy densities exceed that of TiS_2 (480 W h/kg). The latter also needs, for maximum performance, an $LiClO_4$–dioxolane solution which has been recognized to be highly unsafe [43, 44] and cannot be used in practical cells. Other solutions have given less satisfactory results. Among them, the best seems to be the $LiAsF_6$–2-Me-THF developed at the EIC Laboratories [45]. Both TiS_2 and V_6O_{13} were investigated in this solution and the projected energy densities of Li cells as a function of Li utilization are compared in Fig. 8. Higher specific capacities and higher voltages are shown by the oxide. Furthermore, extended cycling in the same solution [2] has shown that both forms of V_6O_{13} behave satisfactorily, with capacities stabilizing, after the initial cycles, near 0.52 e/V for stoichiometric V_6O_{13} and near 0.65 e/V for the non-stoichiometric variety.

However, a significant drawback with both forms of V_6O_{13} is their irreversibility when discharged below *ca.* 1.7 V [2]. This may prevent their use in practical cells. On the other hand, the structurally similar $Li_{\sim 1}V_3O_8$

TABLE 1

Maximum Li$^+$/M and theoretical energy densities for selected Li/oxide couples

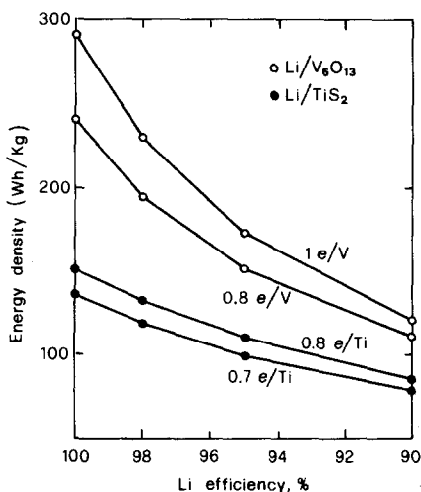| Oxide	Li$^+$/M	W h/kg	Ref.
Cr_3O_8	1.4	1080	47
Li_xCoO_2	0.92	1100	6
V_6O_{13}	1.25	800	23
$Li_{1+x}V_3O_8$	1.0	670	
$(Mo_{0.3}V_{0.7})_2O_5$	1.1	660	25
$Mo_{17}O_{47}$	1.5	490	18

Fig. 8. Projected energy densities for Li/TiS$_2$ and Li/V$_6$O$_{13}$ cells as a function of Li$^+$ utilization (ref. 45).

does not show this drawback, as it has been cycled with voltage limits as low as 1.0 V without any problems.

An interesting application of some reversible oxides offers an alternative to Li electrodes in the so-called rocking chair batteries [10, 40, 46]. For this purpose, the materials are required to incorporate Li$^+$ in good amounts and at low and relatively constant potentials. Ferric oxide seems to possess these requirements, and may give, with V$_2$O$_5$, a couple which, in a battery of the type Li$_6$Fe$_2$O$_3$/LiClO$_4$-PC/V$_2$O$_5$, has an OCV of 3.0 V and may be cycled at 0.5 mA/cm^2 with good efficiencies [46].

6. Conclusions

In the conclusion of his review on intercalation compounds [1], Whittingham prophetically stated that "much effort is likely to be spent on oxide compounds both to understand their insertion compounds and to find those that might be applicable in electrodes for energy storage". This is exactly what has happened in the last 5 years and is expected to continue in the future.

This research has allowed a better comprehension of the thermodynamics and kinetics connected with Li$^+$ penetration within crystalline lattices. A re-evaluation of framework structures with respect to the layered ones has also occurred. Furthermore, within the former class the structural requirements for fast and quantitative Li$^+$ acceptance have been defined.

From a practical standpoint, the challenge to TiS$_2$ is on the way, especially by the V oxides, and could give interesting results.

Acknowledgement

References

1 M. S. Whittingham, *Prog. Solid State Chem., 12* (1978) 41.
2 K. M. Abraham, J. L. Goldman and M. D. Dempsey, *J. Electrochem. Soc., 128* (1981) 2493.
3 D. W. Murphy, P. A. Christian, F. J. DiSalvo, J. N. Carides and J. V. Waszczak, *J. Electrochem. Soc., 128* (1981) 2053.
4 J. O. Besenhard and R. Schöllhorn, *J. Power Sources, 1* (1976) 267.
5 G. Pistoia, C. Temperoni, P. Cignini, M. Icovi and S. Panero, *J. Electroanal. Chem., 108* (1980) 169.
6 K. Mizushima, P. C. Jones, P. J. Wiseman and J. B. Goodenough, *Mater. Res. Bull., 15* (1980) 783.
7 M. Pasquali, G. Pistoia and F. Rodante, *Solid State Ionics, 6* (1982) 319.
8 A. J. Jacobson, *Solid State Ionics, 5* (1981) 65.
9 L. Kihlborg, *Ark. Kemi, 21* (1963) 471.
10 D. W. Murphy, F. J. DiSalvo, J. N. Carides and J. V. Waszczak, *Mater. Res. Bull., 13* (1978) 1395.
11 D. W. Murphy, P. A. Christian, J. N. Carides and F. J. DiSalvo, in P. D. Vashishta, J. N. Mundy and G. K. Shenoy (eds.), *Fast Ion Transport in Solids*, Elsevier, Amsterdam, 1979, p. 149.
12 H.Y.-P. Hong, *J. Power Sources, 5* (1980) 137.
13 D. W. Murphy and P. A. Christian, *Science, 205* (1979) 651.
14 D. W. Murphy, M. Greenblatt, J. Cava and S. M. Zahurak, *Solid State Ionics, 5* (1981) 327.
15 R. J. Cava, A. Santoro, D. W. Murphy, S. Zahurak and R. S. Roth, *Solid State Ionics, 5* (1981) 323.
16 K. A. Wilhelmi, K. Waltersson and L. Kihlborg, *Acta Chem. Scand., 25* (1971) 2675.
17 L. Kihlborg, *Acta Chem. Scand., 21* (1967) 2495.
18 P. A. Christian, J. N. Carides, F. J. DiSalvo and J. V. Waszczak, *J. Electrochem. Soc., 127* (1980) 2315.
19 P. Cignini, M. Icovi, S. Panero, G. Pistoia and C. Temperoni, *J. Electroanal. Chem., 102* (1979) 333.
20 M. Icovi, S. Panero, A. D'Agate, G. Pistoia and C. Temperoni, *J. Electroanal. Chem., 102* (1979) 343.
21 P. Fiordiponti, G. Pistoia, C. Temperoni, M. Icovi and S. Panero, *J. Electroanal. Chem., 108* (1980) 181.
22 P. C. Spurdens, J. Drennan, J. R. Owen, B. C. H. Steele, J. M. Gonzales-Calbet and D. A. Jefferson, *Solid State Ionics, 5* (1981a) 335.
23 D. W. Murphy, P. A. Christian, F. J. DiSalvo and J. N. Carides, *J. Electrochem. Soc., 126* (1979) 497.
24 A. D. Wadsley, *Acta Crystallogr., 10* (1957) 261.
25 P. Fiordiponti, M. Pasquali, G. Pistoia and F. Rodante, *J. Power Sources, 7* (1981) 133.
26 M. Pasquali, G. Pistoia and F. Rodante, *J. Power Sources, 7* (1981) 145.
27 K. H. Cheng, A. J. Jacobson and M. S. Whittingham, *Solid State Ionics, 5* (1981) 355.

28 J. Graham and A. D. Wadsley, *Acta Crystallogr., 14* (1961) 379.
29 K. H. Cheng and M. S. Whittingham, *Solid State Ionics, 1* (1980) 151.
30 B. Di Pietro, V. Filippeschi, M. Lazzari, G. Pistoia and B. Scrosati, in D. H. Collins (ed.), *Power Sources 6*, Academic Press, London, 1977, p. 527.
31 R. G. Burns and V. M. Burns, *2nd Int. Symp. on MnO₂*, The Electrochemical Society (Cleveland Section) Tokyo, 1980, p. 97.
32 H. Ikeda, T. Saito and H. Tamura, *1st Int. Symp on MnO₂*, The Electrochemical Society (Cleveland Section) Cleveland, Ohio, 1975, p. 384.
33 G. Pistoia, *J. Electrochem. Soc., 129* (1982) 1861.
34 T. Kahara, T. Horiba, K. Tamura and M. Fujita, in B. B. Owens and N. Margalit (eds.), *Proc. Symp. on Power Sources for Biomedical Implantable Applications and Ambient Temperature Lithium Batteries*, The Electrochemical Society, Princeton, NJ, 1980, p. 300.
35 M. Voinov, *Electrochim. Acta, 26* (1981) 1373.
36 V. Manev, personal communication.
37 P. G. Dickens and G. J. Reynolds, *Solid State Ionics, 5* (1981) 331.
38 I. D. Raistrick, A. J. Mark and R. A. Huggins, *Solid State Ionics, 5* (1981) 351.
39 P. G. Dickens, S. J. French, A. T. Hight and M. F. Pye, *Mater. Res. Bull., 14* (1979) 1295.
40 M. B. Armand, in D. W. Murphy, J. Broadhead and B. C. H. Steele (eds.), *Materials for Advanced Batteries*, Plenum Press, New York, 1980, p. 145.
41 A. S. Nagelberg and W. L. Worrell, *J. Solid State Chem., 38* (1981) 321.
42 P. G. Dickens, S. J. French, A. T. Hight, M. F. Pye and G. J. Reynolds, *Solid State Ionics, 2* (1981) 27.
43 M. S. Whittingham and J. N. Panella, *Mater. Res. Bull., 16* (1981) 37.
44 G. H. Newman, R. W. Francis, L. H. Gaines and B. M. L. Rao, *J. Electrochem. Soc., 127* (1980) 2095.
45 G. L. Holleck, K. M. Abraham and S. B. Brummer, in B. B. Owens and N. Margalit (eds.), *Proc. Symp. on Power Sources for Biomedical Implantable Applications and Ambient Temperature Lithium Batteries*, The Electrochemical Society, Princeton, NJ, 1980, p. 384.
46 B. Di Pietro, M. Patriarca and B. Scrosati, *J. Power Sources, 8* (1983) 289.
47 J. O. Besenhard and R. Schöllhorn, *J. Electrochem. Soc., 124* (1977) 968.